Volc. Seis., 1991, Vol. 11(5), pp.648–670
Reprints available directly from the publisher

Printed in the United Kingdom

A SOFTWARE PACKAGE FOR EARTHQUAKE DATA PROCESSING: EXPERIMENTAL APPLICATION TO STRONG MOTION RECORDS

E.M. Guseva, A.A. Gusev, and L.S. Oskorbin
Institute of Volcanology,
Far East Division,
USSR Academy of Sciences,
Petropavlovsk-Kamchatskii
Institute of Marine Geology and Geophysics, Far East Division,
USSR Academy of Sciences, Yuzhno-Sakhalinsk

A software package is proposed for processing earthquake records obtained with instruments of various types. It was tested on strong motion records made at Shikotan, southern Kuriles, and Petropavlovsk, Kamchatka. The processing results include acceleration, velocity, displacement, peak acceleration, response spectra, Fourier spectra, and S-wave polarization diagrams. Results are presented for the December 6, 1978, M=7.8, I=VII-VIII earthquake recorded at Shikotan.
(Received April 20, 1988).

Introduction

The USSR Seismic Observation System (ESSN) makes a wide use of S5S seismographs combined with ISO-type and other recorders to record strong motions. Several techniques are available for processing such records (see /2, 3/ for reviews of the literature). However, no technique has been authorized as a standard. In this connection the software package presented here can be useful. It

has been designed, among other things, for processing records of strong motions measured with velocimeters. It can also be conveniently used to process accelerograph and seismograph records obtained with galvanometer and direct recording. The package can also be applied to ordinary seismograms. It is based largely on conventional algorithms of seismic data processing. The package was tested on strong motion records obtained at seismic stations Shikotan, southern Kuriles, and petropavlovsk, Kamchatka, coded here as SKT and PTR. The processing of experimental records yielded some practical seismological findings.

Brief Description of Algorithms and Programs

The software package consists of seven programs. Program 1 computes "true" ground displacement, velocity, and acceleration by a linear inverse filtering of seismic records; Program 2 is an interactive procedure intended to reconstruct the "true" displacement for a unipolar impulse; Program 3 computes a model record for an instrument from a record of another instrument; Program 4 computes response spectra; Program 5 computes unsmoothed Fourier spectra, smooths amplitude Fourier spectra with a constant frequency interval and constant bandwidth, and computes power spectra; Program 6 computes Fourier spectra with smoothing over a log frequency grid, the relative bandwidth being constant; Program computes power spectra by the maximum entropy method (MEM).

Program tasks and applications. The major practical problems that can be tackled by the programs are as follows. Program 1 reconstructs the time variation of ground displacement, velocity, or acceleration from the seismic record. It is particularly efficient for phase correction, for example, in computing acceleration from an accelerogram and displacement from a seismogram. Results are less dependable in reconstructing low-frequency displacement, especially from accelerograms. Under some circumstances better results can be achieved with Program 2.

Although it is far from being versatile, it can in some cases provide reliable estimates of the seismic moment and source function duration.

As a matter of fact, Program 1 is able to compute velocity and acceleration from velocigrams and accelerograms without a rigorous control by the seismologist. The same applies to the computation of displacement from velocity within a fixed frequency band. Computations of acceleration from seismograms, displacement from accelerograms, and the use of Program 2 demand that the user must be skilful enough to know and anticipate potential errors, otherwise results may be misinterpreted.

Program 3 computes a model record for a given instrument from a record available from another instrument. In particular, it is used to reconstruct (from a strong motion record) a model record of a regional seismograph and determine an earthquake energy class.

Program 4 provides a conventional engineering-seismological representation of ground motion in the form of a response spectrum. It should be remembered that the frequency grid is to be consistent with damping. It is not recommended to use a log frequency interval greater than 0.05 when the damping is low (0 to 2 percent). It should also be taken into account that the oscillator model input receives acceleration as a function of time as computed by the program, so that its errors will affect the response spectrum. In particular, one should not hope to obtain reliable results at high frequencies when a record of displacement is used as input for Program 4.

Programs 5, 6, and 7 are designed for various versions of spectral analysis. Program 5 performs standard applications of Fourier analysis, including an ordinary power spectrum estimate and the associated confidence interval. The positions of spectral peaks (resonance in the ground or building) can be refined using Program 7

Program 6 is specially designed for seismological applications

considering that spectra representations on a log-log scale gain increasing popularity in the analysis of seismic signals and noise. The treatment of high frequencies is simplified by using a special algorithm to smooth the Fourier spectrum modulus, the relative band-width and log frequency interval being kept constant. The point of doing so is that the result of such treatment can be directly compared to response spectra and Chiss* (Chiss is the abbreviation of the Russian for frequency-selective seismic system.) -spectra which are derived using the principle of a constant relative bandwidth as well.

The high-frequency portion thus smoothed and the low-frequency portion, where smoothing is infeasible, are linked by the user manually. Note that the smoothing algorithm used in Programs 5 and 6 preserves signal power (energy), being different in this respect from popular algorithms for smoothing the spectrum modulus.

Description of Programs. All programs include a standard initial segment and a special segment. The standard initial segment contains an input module and a conventional processing module. The input module inputs, corrects, and decimates a digitized record and selects intervals to be processed.

The input is first corrected for the displacement and misalignment of the source record baseline that may be caused by digitization. This is done by computing a linear function fitting the baseline and subtracting it from the original samples. The function can be found by any of the following procedures. The first, conventional procedure is to determine, by the least squares method, a straight line that fits the seismogram samples. The second, more primitive, yet more convenient and reliable procedure is to use the baseline level at the beginning and end of the digitized interval to determine the desired straight line. This can be done provided that two portions of the baseline before and after the record segment of interest are digitized. The second procedure is more efficient for short asymmetrical records.

The next procedure performed by the conventional module is to select and "cut out" a segment to be processed. It is executed under the user's control from the display. To avoid "steps" arising at the beginning and end of the segment the initial and final parts of the segment are multiplied by smoothing functions like a half cosine window; for example, the smoothing function for the initial part has the form

$$W(t)=\begin{cases}0; & t<t_1\\ 0{,}5\left(1-\cos\pi\left(\frac{t-t_1}{t_2-t_1}\right)\right); & t_1<t<t_2\\ 1; & t>t_2\end{cases}$$

The lengths of the left (t_1-t_2) and right smoothed parts are entered from the keyboard.

On some occasions records are digitized at short intervals for greater reliability. In such cases they can be decimated using a factor of 2^k and averaging the adjacent samples.

The standard processing module corrects the record for intrumental effects by inverse filtering and selects the desired type of signal (displacement, velocity, or acceleration). Intrumental effects are corrected in the frequency domain by dividing the signal by the instrument transfer function (ITF) which is computed using the parameters of the instrument and the magnifiation at a frequency of interest. As the transfer function for all seismic instruments is close to zero at low frequencies, a high-pass filter is used to reduce low frequency noise associated with division by a small number. The cutoff is chosen so as to reconcile the low frequency noise level and the degree of the source pulse distortion. This operation is only important for displacement computations. The cutoff is selected by the user and entered from the keyboard. In processing seismograms and velocimeter records the natural frequency of the pendulum can be used as a first approximation. This point is considered in greater detail

in /3/.

Apart from low-cut filtering, a high-cut filter is used in some cases, for example, to reduce high-frequency noise or to compare results from instruments of different types. The high-cut filter is also available, its cutoff frequency being also assigned in the interactive mode.

The algorithm of this module actuates successively fast Fourier transform, low-cut and high-cut filtering, divison by the ITF, multiplication by $(i\omega)^K$, with K=0, 1 or 2 for displacement, velocity, or acceleration, respectively, and fast Fourier snythesis, whenever necessary. The subsequent operations vary from one program to another. They are described below in the order of the list of programs above.

(1) Displacement, velocity or acceleration time functions are displayed. The original record can be displayed, too.

(2) An interactive procedure of computing the "true" ground motion is performed. Details are to be found in /3/; it is used here practically unmodified. We are going to give brief explanations of this program. Inverse filtering in a restricted frequency band outside zero may produce low-frequency distortions in the reconstructed ground displacement. The distortions can sometimes be compensated, provided there is a priori information on the signal. The algorithm described in /3/ can be used to reconstruct signals having the shape of unipolar impulses. The body waves that are excited by a dislocation source in a uniform isotropic medium must have this shape. The idea of the algorithm is to extrapolate the signal spectrum into the vicinity of zero. Where a unipolar source impulse is reliably identified, the program determines its area E_o and normalized power moments, the first initial e_1 and the second central e_2, as given by

$$E_0 = \int_{t_A}^{t_B} x_u(t)\,dt,$$

$$e_1 = \frac{1}{E_0} \int_{t_A}^{t_B} x_u(t)(t - t_A)\,dt,$$

$$e_2 = \frac{1}{E_0} \int_{t_A}^{t_B} x_u(t)(t - t_A)^2\,dt - e_1^2,$$

where t_A, t_B are the times of the beginning and end of the impulse, $x_u(t)$ is the estimated source impulse. The impulse area E_o which is equal to the modulus of the Fourier spectrum at zero frequency can be used to estimate the seismic moment M_o.

A module for computing spectral corrections for attenuation was added to study earthquake sources. One should fix travel time and Q as a function of frequency to compute the correction. Amplitude correction is computed in a straightforward manner. Phase correction is computed as the Hilbert transform of the log modulus of the amplitude correction, thus ensuring that the operator of the medium is physically realizable /5/.

(3) The displacement spectrum is multiplied by the transfer function of the instrument modelled, the instrument parameters being fixed by the user. The fast Fourier synthesis is performed and the model record is displayed.

(4) To compute a response spectrum, the time behaviour of displacement under a given acceleration is modelled for a set of dimensionless damping D values and natural frequency ω_0 of the mechanical oscillator. A set of absolute values of peak displacement X as a function of ω_0 yields the displacement spectrum (for D fixed); one can also obtain pseudovelocity $V(\omega_0) = \omega_0 X(\omega_0)$ and pseudoacceleration $A(\omega_0) = \omega_0^2 X(\omega_0)$ spectra. The oscillator motion is modelled by time series approach using a recursive filter of degree five. The filter coefficients are found from the formulas given in /9/. The response spectrum for a given set of D values is displayed in a log-log scale.

(5) Two plots are displayed, both in the same log linear scale. One shows the unsmoothed modulus of Fourier spectrum

(displacement, velocity, or acceleration). Then the power spectrum is computed as the square of the modulus of Fourier spectrum over a fixed uniform frequency grid (at a constant interval) and smoothed using a cosine window of fixed width. The window width is typically (for -3 dB) twice the frequency interval. The smoothed result can be regarded as a power spectrum estimated to an accuracy of a constant factor. The smoothed amplitude Fourier spectrum is found by taking the square root; it is displayed as the second plot. Note that, since the scale along the ordinate is logarithmic, taking the square root does not affect the spectral curve shape.

(6) Two plots are displayed, both in the log-log scale. One shows the unsmoothed modulus of Fourier spectrum (displacement, velocity, or acceleration). A smoothed Fourier spectrum is then computed in about the same way as in Program 5, except that the frequency grid for which the values of a smoothed spectrum are computed has a constant log frequency spacing instead of being uniform. Accordingly, the width of the smoothing window is no longer constant either, the relative width being constant. For the estimate at frequency f, the recommended (absolute) half-width at -3 dB level should be $\delta f = \frac{1}{2} f(10^{\Delta} + 10^{-\Delta})$, where Δ is a log frequency interval (and a half-width on a log scale). For example, if the frequency grid contains 10 points per decade, then Δ=0.1 and $\delta f = 0{,}23 f$. The values of smoothed spectrum are not computed for low enough frequencies, because the smoothing window must contain at least two or three values of the unsmoothed spectrum. The computed unsmoothed values are displayed as the second plot.

(7) This program implements the maximum entropy method (MEM) after /5/ except that the algorithm is upgraded for the results to have the sense of a power spectrum. The MEM-estimated power spectrum and the unsmoothed power spectrum obtained by a discrete Fourier transform, both on a log-log scale, are displayed.

Database.

Table 1. Earthquakes Recorded at Station SKT

Date	T_0, hour min, sec	φ° N	λ° E	h, km	Δ km	R, km	K	M	I, intensity	Record number N-S	Record number E-W
May 8, 1981	06.44.50,0	44,6	146,4	165	95	190		5,8*LH*	2	A18	A17
Aug 4, 1981	22.45.14,0	44,0	147,1	90	30	95	10			A5	A4
Sept 8, 1981	19.26.28,0	43,4	146,4	48	55	73	12	5,7*LH*	3	A19	—
Oct 3, 1981	07.21.50,0	43,8	146,6	75	15	76	10,5	5,1*PV(A)*	4—5	A8	A6
Nov 13, 1981	19.35.10,0	43,5	146,5	60	65	88	11	5,4*PV(A)*	5	A14	A13
July 4, 1981	14.51.56,0	43,9	146,8	90	10	91	10,5	—	4	A11	A9
Aug 30 1982	06.27.16,0	44,6	147,4	90	90	127	10,5	—	—	A16	A15
Oct 22, 1982	02.28.40,0	43,5	146,7	50	40	64	10	—	4	A3	A2
Dec 6, 1978	14.02.05,0	44,6	146,64	140	82	162		7,5*LH*	7—8		

Table 2. Earthquakes Recorded at Station PTR

№	Date	T_0, hour min, sec	φ°	λ°	h, km	Δ, km	S–P, s	F68 $K_{S1,2}$	M
1	Apr 12, 1973	13.49.14,5	50,70	158,88	70		28	14,8	$m_{PV(A)}$=6,2
2	July 11,1975	05.23.22,8	53,28	159,00	115		13	11,7	$m_{PV(A)}$=5,0
3	Feb 11, 1980	15.29.47,0	53,12	160,05	57		12	12,7	M_{LH}=4,4
4	Oct 13, 1981	15.33.57,4	51,35	157,71	101		23	12,9	$m_{PV(A)}$=5,3
5	May 14, 1982	03.38.03,5	52,55	158,31	121		14	11,9	m_b=5,0
6	Feb 1, 1987	04.11.35,2	52,91	158,94	100		11	12,1	$m_{PV(A)}$=4,8
7	Nov 24, 1971	19.35.49,0	52,50	162,20	100	120	—	16	M_{LH}=7,2
8*	—	—	52,42	160,05	10—30	102	—	14	—

*Record No.44 from /7/, without inverse filtering

The velocigraphs at stations SKT and PTR produce ordinary galvanometer photographic records. The S5S-N700 seismograph at SKT has two sensitive horizontal seismometers with the sensitivity V=5 s, two low-sensitivity horizontal seismometers with V=0.5 s, a vertical seismometer with V=0.5 s, and a time marker. It produces galvanometer records on 12-cm photographic chart at a drum speed of 20 mm/s. At it is triggered by the first arrival, it is only S waves that are recorded without gaps.

In this experiment we used records of earthquakes recorded at station SKT in 1981 and 1982 with magnitudes M_{LH} in the range 5-6. We chose shocks with focal depths of 50 to 120 km (Tables 1 and 2, Fig.1) and hypocentral distances of 60 to 200 km. This choice was determined by our interest in the identification of undistorted source displacement impulses. We know from the previous work with P waves that this could only be expected in the case of steep enough rays. It should be noted that our hopes of identifying S-wave source impulses have only partially realized. We also records of the SSRZ accelerograph at station SKT and records of the S5S-ISO-2 seismograph at station PTR. All records digitized using a UTsS (FOO4) digitizer. We digitized large-amplitude portions in horizontal records which contained S waves. The sample interval was Δt=0.004-0.1 s.

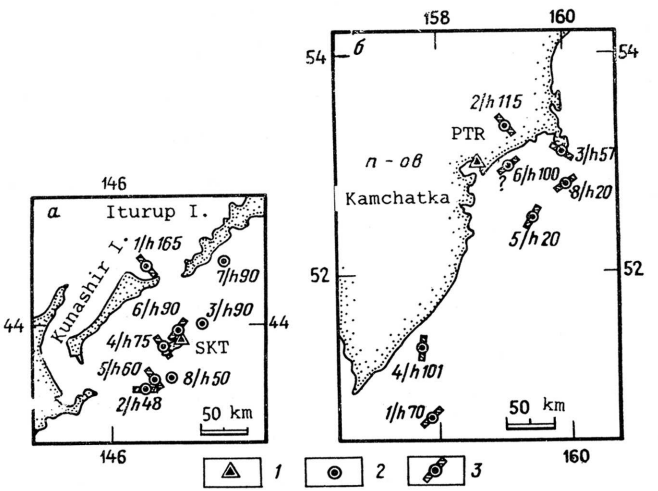

Fig.1. Location map of earthquake sources: a - SKT station area; b - PTR station area. 1 - seismograph station; 2 - epicentre; 3 - epicentre and the direction of faster S-wave polarization. Earthquake numbers are as given in Tables 1 and 2; h - depth of focus .

Results of Experiment

Testing procedure. Velocimeter records of moderate shocks were used to test Programs 1, 2, 4, and 6. The testing results are

outlined below successively; also, some seismological interpretations are given, largely by way of illustration. Records of large earthquakes were processed by Programs 1, 4, and 6. The results of testing Program 2 can be found in /2, 3/ and those of Program 3 in /4/. Results of testing Programs 5 and 7 are not presented. The standard procedure common to all programs was the reconstruction of the input signal. It was performed in the frequency range 0.2-0.3 Hz to 15-30 Hz. The upper cutoff was determined by the sampling rate which was in turn chosen with an eye to actual "ruggedness" of the record. We nearly always had at least six points per the shortest apparent period. The lower cutoff was chosen depending on the natural pendulum frequency (0.2 Hz).

Displacement, Velocity and Acceleration. Fig.2 presents examples of reconstructed displacements, velocities, and accelerations for records at station SKT. The record length was limited by the computational and plotting facilities of the computer. The original velocimeter records and the reconstructed velocity curves are superposed. The amplitudes of the curves show a close fit, as would be expected, the small discrepancies being due to phase correction. We remind the reader that the phase response of a real velocigraph is non-linear. The reconstructed records of acceleration, velocity, and displacement were used to determine their peak values (a, v, x) and those of velocity and acceleration yielded apparent periods (T_v, T_a). The results are summarized in Table 3. The order of entries in Table 2 corresponds to Table 1.

Fig.3 presents, for most of the records processed, the original velocigrams, the displacements reconstructed by linear inverse filtering and, wherever possible, the reconstructed displacement impulses (see description of Program 2). The comparison of plots A2 and A3 shows that the use of a priori information of the signal eliminates distortions in the displacement curves that have been reconstructed by linear inverse filtering.

A few comments need be made concerning Fig.3. First, we

expected, following Booth and Crampin /10/, that S-wave polarization for steep rays (angles of emergence below 35-40°) would be approximately linear at an isotropic free surface, even with the wave front curvature taken into account. Second, from the experience of P wave study under similar conditions /2/ we expected that the records would contain unipolar S wave impulses corresponding to a standard dislocation source model. Both of these expectations have failed to realize. Fig.3 shows that the waveforms on the two components are markedly different, and that a unipolar impulse can be identified in one record and on one component only.

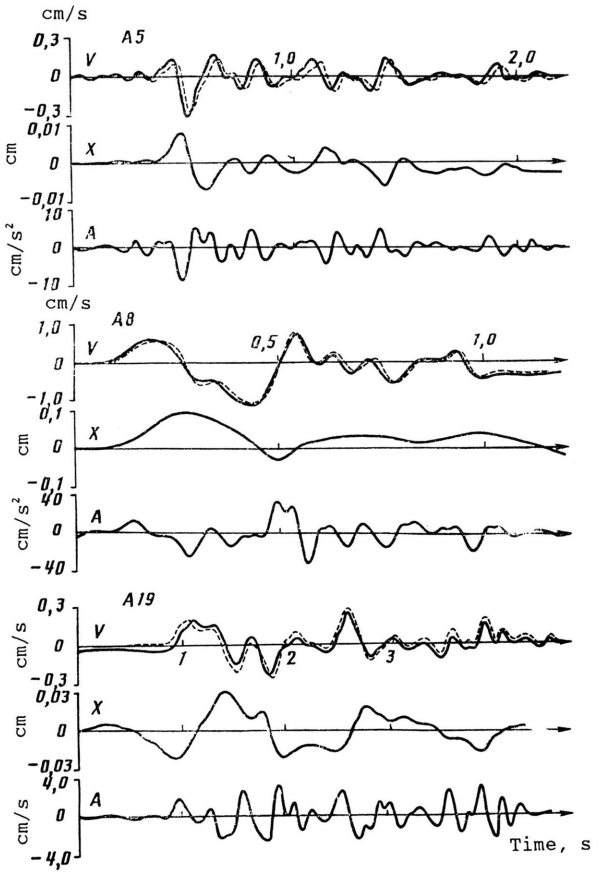

Fig.2. Examples of reconstructed displacements (X), velocities (V), and accelerations (A) for earthquake records made at station SKT. the dashed line is the original velocigram; A5, A8 and A19 are numbers of records as given in Table 1.

In this situation we found it reasonable to carry out a polarization analysis with the view of detecting anisotropic effects. On the other hand, unipolar impulse could be used to roughly estimate seismic moments and source function duration.

Table 3. Characteristics of Earthquake Records at Station PTR

Component	V, cm/s	T_v, s	a, cm/s^2	T_a, s	x, cm	S, cm/s	log M_o, dyne. cm
North-south	0.12	0.45	2.4	0.12	0.007	$0.33 \cdot 10^{-2}$	23.22
North-west	0.09	0.25	2.6	0.09	0.006	$0.31 \cdot 10^{-2}$	23.14
North-south	0.23	0.16	9.2	0.11	0.009	—	—
East-west	0.3	0.1	12.8	0.13	0.009	$0.47 \cdot 10^{-2}$	23.07
North-south	0.20	0.3	2.88	0.33	0.025	$0.71 \cdot 10^{-1}$	23.13
East-west	—	—	—	—	—	—	—
North-south	0.86	0.35	25.2	0.14	0.064	$0.21 \cdot 10^{-1}$	23.63
East-west	0.47	0.3	13.4	0.10	0.035	$0.14 \cdot 10^{-1}$	23.46
North-south	0.27	0.14	11.5	0.12	0.015	$0.89 \cdot 10^{-2}$	22.96
East-west	0.30	0.14	16.0	0.12	0.017	$0.60 \cdot 10^{-2}$	22.78
North-south	0.40	0.14	13.6	0.12	0.012	$0.23 \cdot 10^{-2}$	22.73
East-west	0.39	0.09	18.4	0.1	0.011	$0.25 \cdot 10^{-3}$	21.89
North-south	0.06	0.19	1.38	0.19	0.018	—	—
East-west	0.07	0.19	3.52	0.14	0.002	—	—
North-south	0.51	0.25	16.0	0.10	0.032	$0.10 \cdot 10^{-1}$	22.88
East-west	0.62	0.18	18.0	0.18	0.024	$0.41 \cdot 10^{-2}$	22.47
North-south	8.0	0.19	205 (154)*	0.14	—	—	—
East-west	17.6	0.45	320 (312)*	0.18	—	—	—

*Parenthesized is peak acceleration found from the accelerogram

S-wave polarization from data recorded at station SKT.

Displacement curves in Fig.3 were used to plot ground motion paths in the horizontal plane (Fig.4). The plots in Fig.4 are based on the record segments between the dots in Fig.3. None of the records except one show linear polarization. Moreover, following /11/ one can envisage in some records the arrival of a slower wave polarized perpendicularly to the direction of the first, faster S wave. This may be indicative of anisotropy under the SKT site. We tried to learn more about the anisotropy by determining the approximate

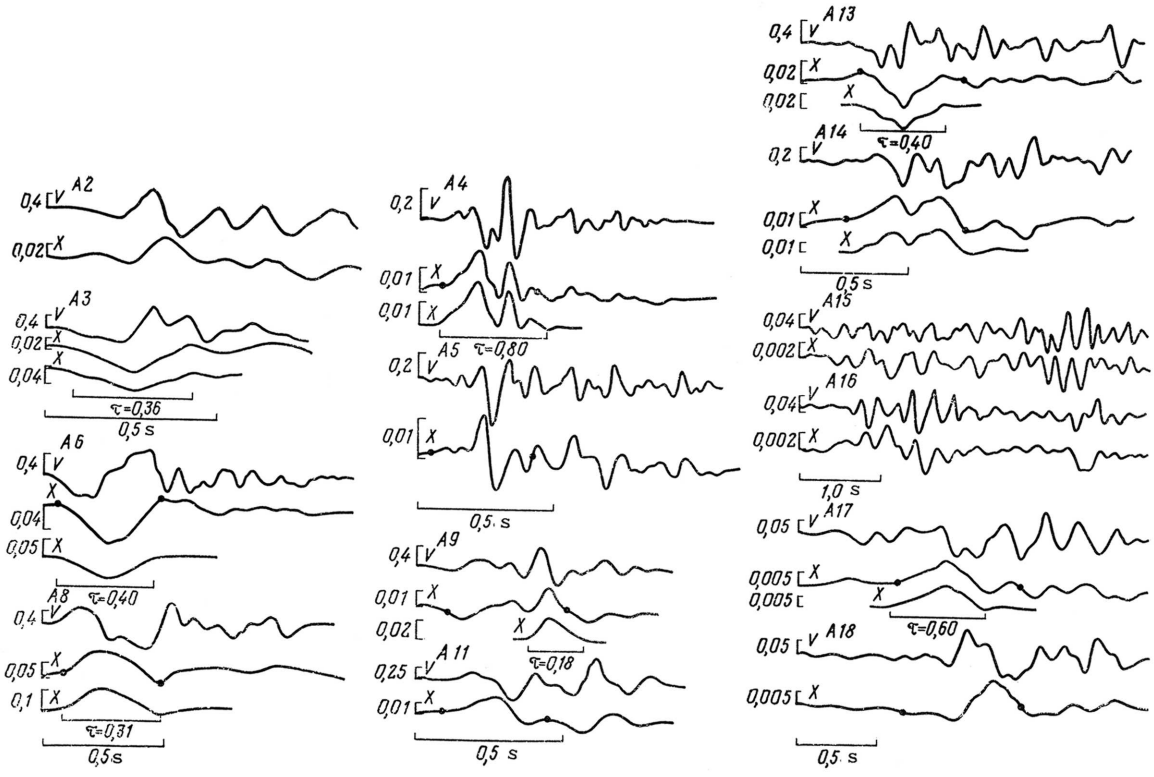

Fig.3. Original velocigrams (V, cm/s), displacement functions reconstructed by the spectral method, and estimated displacement impulses (X, cm) for earthquakes recorded at station SKT. τ - impulse duration, in s. Dots enclose the record segments for which ground motion paths are given in Fig.4. the numbers of records are same as in Table 1.

direction of the faster wave polarization from the curves of Fig.4 and plotting the results on the map of Fig.1. Even though the data are scarce, this pattern does not seem to be accidental and the direction of the fast S-wave polarization is likely to be perpendicular to the island arc.

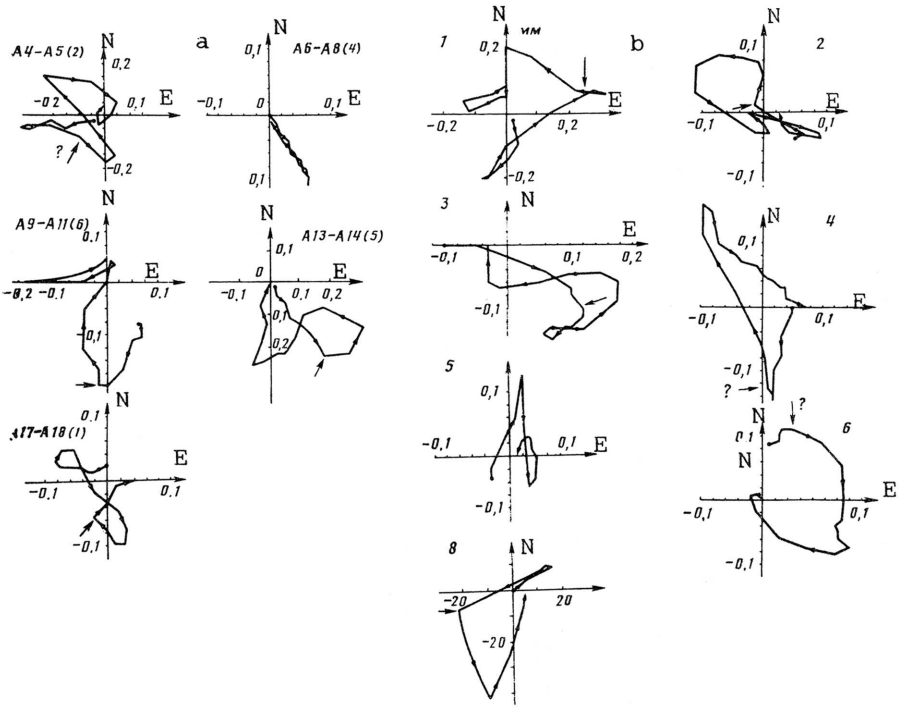

Fig.4. Ground motion paths in the horizontal plane; a - at station SKT; b - at station PTR. Plot number refers to earthquake number in Table 1 for SKT and in Table 2 for PTR. Arrows indicate approximate times of arrival for the slower wave.

S-wave polarization from data recorded at station PTR.

Differences in S-wave polarization under the PTR site were reported earlier /7/. We have studied that phenomenon using S-wave records obtained at station PTR with an S5S-ISO seismograph. The parameters of the events are summarized in Table 2. The horizontal directions of displacement in the faster S wave are

shown in Fig.1. Also shown in the figure (see 8/h20) is the polarization of record 44, the only one that was suitable for the purpose among the records presented in /7/. It should be noted that the earthquakes 1, 3 and 4 are subcrustal, and the angles of emergence for them are low owing to ray path curvature. Although there is some regularity, no clear-cut pattern emerges. It seems there exists a boundary between blocks of contrasted anisotropy to the northeast of PTR. This idea finds support in the fact that polarization for earthquake 6 with a low angle of emergence is elliptic rather than linear, though a homogeneous anisotropic model would yield a well-defined linear polarization near the S arrival.

The problem of anisotropic structure under SKT and PTR certainly requires more extensive material. Even as it is, however, we may say that the earth under these stations, and probably under other island-arc areas, is notably anisotropic. Under these circumstances the S waveform can be considerably distorted even in the case of nearly vertical ray paths. The distortions include, first, a nearly invariable loss of S wave form correlation between the two horizontal components and, second, distortions of shape, up to the loss of the typical unipolar form, for the presumed unipolar impulse radiated at the source. At the same time, P waves recorded at PTR show well-defined unipolar impulses for angles of emergence below 40°. This difference is important in terms of methodology.

Seismic moment. Seismic moments M_o were computed through the determination of the area of the displacement impulses by Program 2 which yielded impulse duration as a side result. For a source in the crust or mantle M_o was found by the inversion formulas /1/:

$$S_0 = \frac{R^S M_0}{4\pi\rho_K c_K^3 r},$$

$$S_0 = -\frac{R^S M_0}{4\pi\rho_K^{1/2} c_K^{1/2} \rho_M^{5/2} c_M^{5/2} r},$$

where ρ_c, ρ_m and c_c, c_m are density and S wave velocity in the crust and mantle; R^S is the directivity graph; r the hypocentral distance; and S_o the level of displacement spectrum (total vector) of S wave impulse at zero frequency. S_o was found as $S_1.k_1.k_2$ where S_1 is the impulse area on the seismogram, k_1=0.5 is the correction for free surface, and k_2= $\sqrt{2}$ is the correction for the total displacement vector being projected onto the direction of seismometer oscillation. R^S was taken to be $(2/5)^{0.5}$, the mean square directivity of a focal sphere. We used ρ_c=2.7, ρ_m=3.3, c_c=3.5, and c_m=4.7. No correction for attenuation was made. The values of S_o and log M_o are given in Table 3.

Fourier and response spectra. Amplitude Fourier spectra (for acceleration) and response spectra (for velocity) were constructed for the processed S wave records at SKT (Fig.5). The curve of a Fourier Spectrum (without the attenuation correction) consists of two portions, the left being an unsmoothed Fourier spectrum and the right smoothed over a log frequency grid with a bandwidth of 0.1 decade. The relative bandwidth at -3 dB level is $\delta f/f_o = 0.23$, where f_o is the central frequency and δf the half-bandwidth. The grid spacing was also 0.1 decade. The left and right portions are joined at the point marked with a solid circle. The position of the junction is determined by the requirement that only 2 or 3 spectrum points fall within the smoothing window. The lower-most curve is an averaged acceleration spectrum with f_{max} being about 8 Hz.

As acceleration Fourier spectra and velocity response spectra are known to be similar to some extent in shape and level, we present in Fig.5 a response spectrum for one record only, as an illustration, and an averaged response spectrum based on all records. The response spectrum was calculated for 5 percent damping. The grid of frequencies (free oscillator periods) was spaced 0.1 decade, as in the case of smoothing Fourier spectra, (0.100, 0.126, 0,158, 0,200,... Hz.

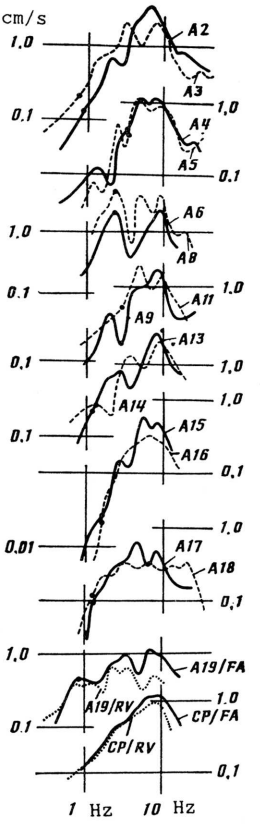

Fig.5. Acceleration Fourier spectra for SKT records. Solid lines are spectra for the east-west component, dashed lines are for north-south on the same seismogram. Numbers of records are given as in Table 1. The left portion of the spectral curve represents the unsmoothed amplitudes Fourier spectrum and the right is the spectrum smoothed over a logarithmic frequency grid. Dots mark places where the two portions are joined. The solid line in the lowermost graph is the averaged acceleration spectrum (CP/FA); the dotted line is the velocity response spectrum averaged over all records (CP/RV). The graph above it compares FA and RV spectra for single record.

Record of the 1971 Petropavlovsk Earthquake. A valuable

record has been obtained with an S5S-ISO-S siesmograph at station PTR of the November 25, 1971, M_{LH}=7.2 ($M_W \approx 7.6$) earthquake at a hypocentral distance of about 120 km /8/. One trace of that record (north-south) was published by Shteinberg et al /8/ together with its Fourier spectrum. We made an attempt to determine peak acceleration from it.

Regrettably, the earth tremor of about intensity VI and large galvanometer amplitude prevented the ISO-2 recorder from producing a satisfactory record. Two kinds of defacts were detected. Inadequate beam brightness resulted in the loss of short record segments in the region of maximum amplitudes. The breaks on the north-south trace were interpolated and those on the east-west totalling about 0.5 s were lost (out of 20-30 s of strong motion record). The other defects were caused by many 0.1-0.2 s stops of the drum driver. They can be identified as steps in the main trace and as dots of increased brightness in the time mark trace, the time marks themselves being shortened in such cases. The steps in the velocimeter record made it impossible to reconstruct the acceleration function with certainty. The steps and drum stops also caused some distortions in the relevant Fourier spectra, but they where too small to effect the integrated spectra.

Fig.6 a, b presents Fourier spectra and response spectra for the N-S and E-W traces. The lost segment of the E-W trace was smoothly inerpolated. The reliabilities of spectra for the two components are comparable. Like in Fig.5 the unsmoothed spectrum is represented in the low-frequency region and the spectrum smoothed over a logarithmic grid at high frequencies.

Record of the December 6, 1978, Southern Kuriles Earthquake. The record of that large earthquake obtained with a standard SSRZ accelerograph has not been published. Fig.7 presents curves of reconstructed acceleration and velocity and Fig.6 c, d Fourier and response spectra, all for the horizontal components. The parameters of the records are given in Table 2.

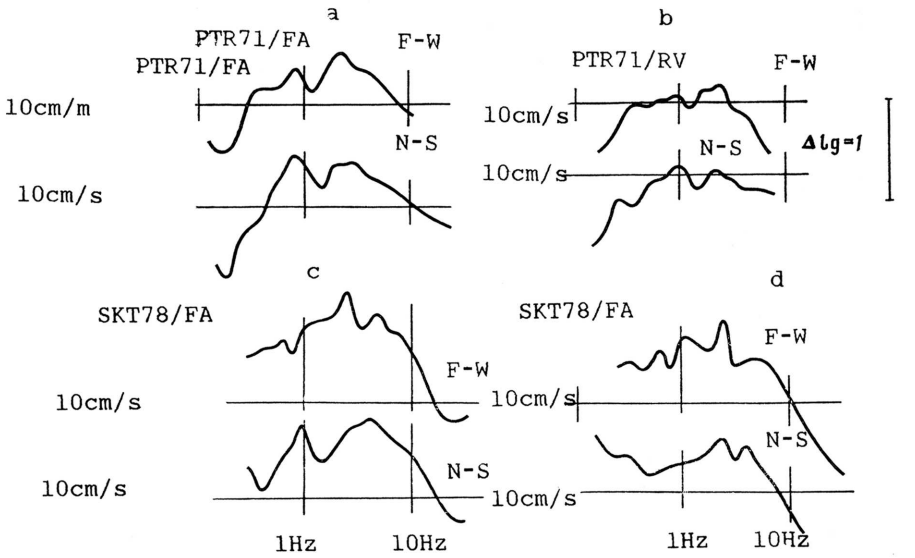

Fig.6. Acceleration Fourier spectra (FA) and velocity response spectra (RV) for the records of two large earthquakes: November 24, 1971 recorded at station PTR: a - FA, b - RV, and December 6, 1978 recorded at SKT: c - FA, d - RV.

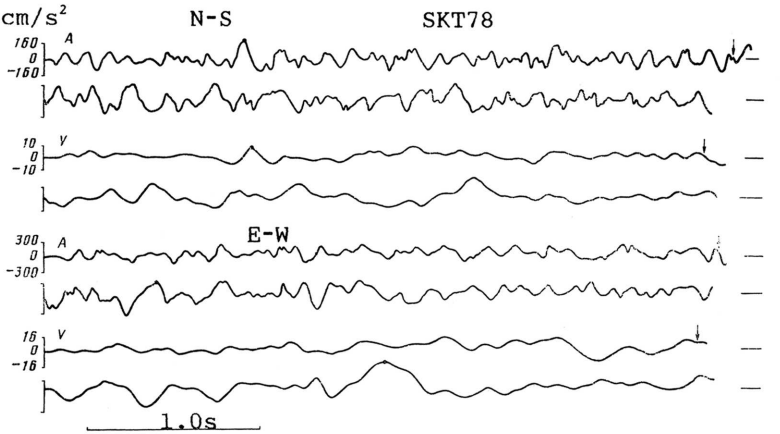

Fig.7. Reconstructed acceleration (A) and velocity (V) for the December 6, 1978 event recorded at station SKT. The graphs are divided into segments which slightly overlap. Dots mark peak values.

Discussion and Conclusions

This experiment proved the software package to be efficient for the analyses of strong motion records obtained with S5S-ISO seismographs of the ESSN network. The following procedures can be performed on a conventional basis: computation of acceleration, velocity, and displacement (frequencies below 0.2-0.3 Hz being filtered); determination of peak acceleration, computation of unsmoothed and smoothed (over a logarithmic grid) Fourier spectra; and computation of velocity response spectra with 5 percent damping. The software is also quite suitable for processing mechanical, optical and galvanometer records of accelerographs and seismographs. The programs are written in FORTRAN, RAFOS OS, and designed for an SM-3 computer. A larger computer is needed to process large quantities of data.

Important results were obtained in terms of practical seismology. A type shape of an acceleration Fourier spectrum and a response spectrum was determined for records of moderate mantle events (intensity III to V, M_{LH}=5-6, r=50-100 km) at station Shikotan. As a matter of fact, it is the first estimate of a spectral shape for hard rocks in the southern Kurile Islands. The engineering seismological parameters of near-zone records from two $M \approx 7.6$ earthquakes were determined. Data were obtained for the magnitude-seismic moment and typical time-seismic moment correlation for the southern Kuriles. The S-wave polarization study revealed that anisotropy was likely to be present under the SKT and PTR sites. Methodological conclusions were drawn concerning the use of S waves in earthquakes source studies; S wave impulses radiated by earthquake sources at 50-100 km depths cannot be reliably reconstructed from records near the eipcentres. This aggravates the situation for the computation (not estimation) of the seismic moment and for detailed study of the source process for such events based on records obtained in the epicentral zone. on the other hand, anisotropy can obviously be studied in detail

using digital or digitized S wave records. In the experimental work reported in /10, 11/ polarization analysis was made using digital readings of velocigraphs. As far as our experience goes, the use of reconstructed displacement (with phase correction) appreciably improves the resolution of polarization diagrams and provides a more reliable identification of the arrival of the slower wave.

Lastly, if the effect of anisotropy on S wave shape is systematically as great as our limited data suggest, this raises the question of reliability for earthquakes mechanism determinations based on S waves in these conditions (namely, mantle events in an island arc, data from local short-period seismograph stations).

REFERENCES

1. K. Aki and P. G. Richards, Quantitative Seismology. Theory and Methods. Vol.1, W.H. Freeman and Company, San Francisco, 1980.
2. A. A. Gusev and E. M. Guseva, in: Physics of seismic waves and the internal structure of the Earth, 15-26, Nauka, Moscow, 1983.
3. A. A. Gusev and E. M. Guseva, Volcanology and Seismology, No.5, (1986).
4. V. M. Zobin, S. A. Fedotov, E. I. Gordeev et al., Volcanology and Seismology, 1, (1988).
5. J. F. Claerbout, Fundamentals of Geophysical Data Processing with Applications to Petroleum Prospecting, McGraw-Hill, New York, 1976.
6. A. G. Moskvina, in: Physics of seismic waves and the internal structure of the Earth, 55-65, Nauka, Moscow, 1983.
7. V. V. Shteinberg, in: Vibrations of earth dams, 123-150, Nauka, Moscow, 1967.
8. V. V. Shteinberg, V. M. Fremd, and V. D. Feofilaktov, in: Large Kamchatka earthquakes in 1971, 7-14, Nauka, Vladivostok: 1975.
9. P. R. Beaudet and S. J. Wolfson, Bull. Seismol. Soc. Amer. 60, 3, 1001-1014 (1970).

10. D. C. Booth and S. Crampin, Geophys. J.Roy. Astr. Soc. 83, 31-45, (1985).

11. S. Crampin and R. Evans, Geophys. J. Roy. Astr. Soc. 83: 31-45, (1985).